Article

Effect of Modifiers on the Disintegration Characteristics of Red Clay

Baochen Liu [†] , Haofeng Zhou, Xiaobo Wang, Guan Lian * and Bai Yang [†]

School of Architecture and Transportation Engineering, Guilin University of Electronic Technology, Guilin 541004, China; bc0608@163.com (B.L.); 18377652778@163.com (X.W.)

* Correspondence: lianguan@guet.edu.cn; Tel.: +86-0773-2303796

[†] These authors contributed equally to this work.

Abstract: Due to the high degree of weathering, the red clay slope has low anti-disintegration performance, and the clay easily becomes wet and disintegrates after soaking in water. It causes geological problems such as slope collapse caused by soil softening. To study the disintegration characteristics of modified red clay, the disintegration test of red clay modified by using lignin fiber, clay particles and lime was carried out, analyzing the disintegration characteristics of improved red clay from physical and chemical perspectives and analyzing the improvement mechanism of three modifiers with the scanning electron microscopy test. The analysis results show that the water-holding capacity and disintegration resistance of soil mixed with lignin fiber decrease; the disintegration time of reshaped red clay increases with the increase in clay content; and the average disintegration rate of the soil decreases with the increase in clay content. With the increase in lime content, the soil cement increases. The integrity of the soil is enhanced, and its anti-disintegration ability is improved; the saturated moisture content of reshaped red clay increases with the increase in lignin fiber and clay content, while the saturated moisture content of soil decreases with the increase in lime content. The damage analysis shows that the larger the damage factor of soil, the worse its anti-disintegration ability, and the easier the soil disintegrates. The purpose of this paper is to explore the essence of the soil disintegration phenomenon, and on this basis, using high-quality improved materials, to improve the soil, which easily disintegrates. This move aims to significantly enhance the anti-disintegration ability of the soil, thereby improving its resistance to softening and disintegration, thereby effectively improving and maintaining the ecological environment. At the same time, the improved soil will help to improve the utilization rate of the slope and foundation soil, thereby reducing the economic cost of maintenance engineering. Against the current background of sustainable economic, social, and ecological development, it is of great strategic significance to ensure the sustainable availability of land resources in specific areas and maintain their productivity and ecological stability for a long time. The research into this subject not only helps to deepen the understanding of soil disintegration, but also provides strong technical support for the rational utilization of land resources and the protection of the ecological environment.

Keywords: red clay; disintegration characteristics; lignin fiber; clay; lime; sustainable development

1. Introduction

With the rapid development of the economy and the Western development strategy in recent years, a growing number of engineering constructions have been constructed in the red clay region. Red clay is widely distributed in China. Aa a special soil, the physical and mechanical properties of red clay are completely different under drying and soaking conditions [1]. Red clay contains a high proportion of hydrophilic minerals, so under the action of water, red clay is prone to disintegration, resulting in the loss of stability of soil structure and the decrease in strength [2]. The mechanical properties of red clay decrease rapidly under soaking conditions, which causes the local softening of the soil, and the

integrity of the soil decreases. In rainy weather, the red clay subgrade often collapses and causes landslides, which causes serious economic losses. To make better use of red clay in engineering, it is of great significance to study its disintegration.

Numerous achievements have been made in the study of the disintegration of rock-soil. There is a significant relationship between the disintegration of clayey soil and its internal clay minerals. These minerals are extremely hydrophilic. Once soaking in water, clay minerals and soluble minerals react with water [3], resulting in soil softening. After experiencing the process of dehydration and drying shrinkage, the moisture absorption pressure of rock and soil will increase accordingly. When the dry rock mass is in contact with water molecules, these water molecules will be driven by the moisture absorption pressure and penetrate along the fracture channels inside the rock and soil. With the infiltration of water molecules, the air originally existing in the cracks and pores of the rock will be gradually compressed. As the amount of water infiltrated increases, the air pressure in the internal pores will gradually increase, which may eventually lead to the collapse and disintegration of the mineral skeleton of the rock and soil in the weak stress area [4]. The difference in mineral composition of the rock–soil can cause uneven expansion, resulting in uneven internal force and cracks [5]. A feasible way to improve the structure and strength of soil is to enhance the water stability by adding modifiers to the soil [6]. The fiber can increase the substrate suction of soil, affecting the pore size of soil to a certain extent. And the fiber can change the pore structure and improve the water stability of the soil [7–11]. The influence of the effective porosity and substrate suction of soil on its disintegration characteristics is positively correlated. The average disintegration rate of soil increases with the increase in effective porosity [12]. The substrate suction of unsaturated soil affects the water seeding rate in soil. The entry of water makes the air in the pores of the soil escape. It causes and internal and external pressure difference, which in turn affects the disintegration of the soil [13].

In summary, different types of soil modifiers affect the spatial structure of the soil through the interaction between modifiers and soil, thereby changing the mechanical properties of the soil [14]. At present, the scholars working on soil improvement mainly focuses on enhancing the shear and compressive strength of soil in the soil slope research field [15–17]. The soil–water characteristic curve was not studied from the perspective of a soil–water relationship. And there are few studies on the disintegration characteristics of red clay by adding modifiers. Therefore, in this paper, the series of disintegration tests on red clay was conducted by adding three modifiers of lignin fiber, clay, and lime. The modification mechanism was analyzed microscopically by an electron microscope scanning test. The influence of three modifiers on the disintegration characteristics of reshaped red clay were analyzed and are discussed in the test results. These provides theoretical guidance for the construction of red clay as engineering material. The research into this subject not only helps to deepen the understanding of soil disintegration, but also provides strong technical support for the rational utilization of land resources and the protection of the ecological environment.

2. Materials and Methods

2.1. Experimental Materials

The test soil is taken from the red slope of Huajiang Village, Lingchuan County, Guilin City, Guangxi Zhuang Autonomous Region (E 25°18′53″, N 110°25′0″). The rock slope is weathered and broken, and the color is reddish brown. The soil is mixed with gravel, and the soil layer is loose. The soil sample was dried in the sun and ground through a 2 mm geotechnical sieve. The basic physical properties of test soils are measured according to the current "Standard for soil test method" [18]. The test results are shown in Table 1. The main mineral composition and quality fraction of test soil were determined by X-ray diffraction analysis and energy spectrum analysis, as shown in Figure 1. The powder XRD patterns were recorded on a diffractometer Rigaku Ultima IV. Radiation was used in the range 2θ 5–80, step 0.02° 2θ, and exposure time per step 0.15 s. The detection is

based on the X-ray diffraction analysis method SY/T5163-2018 [19] of clay minerals and common non-clay minerals in sedimentary rocks. The JADE 6.5 software was used for the phase identification. The specialized software JADE 6.0 was used for qualitative and semi-quantitative phase composition determination. In this study, a tungsten filament snapping bird electron microscope (model: KYKY-EM6200) manufactured by Beijing Zhongke Keyi Co., Ltd. (Beijing, China) was used. The scanning electron microscope test parameters were the following: magnification 2000 times, electron beam voltage 15 V, working distance 12 mm, medium scanning speed, and electron beam current less than 200 mA. The content of hydrophilic minerals in red clay is higher, and the mineral content is 38.7%. The phase composition determined by XRD contains quartz: 51.6%, montmorillonite: 20.1%; goethite: 9.6%; illite: 4.57%; kaolinite: 4.22%; vermiculite: 8.09%; and chlorite: 1.7%.

Table 1. Physical parameters of red clay.

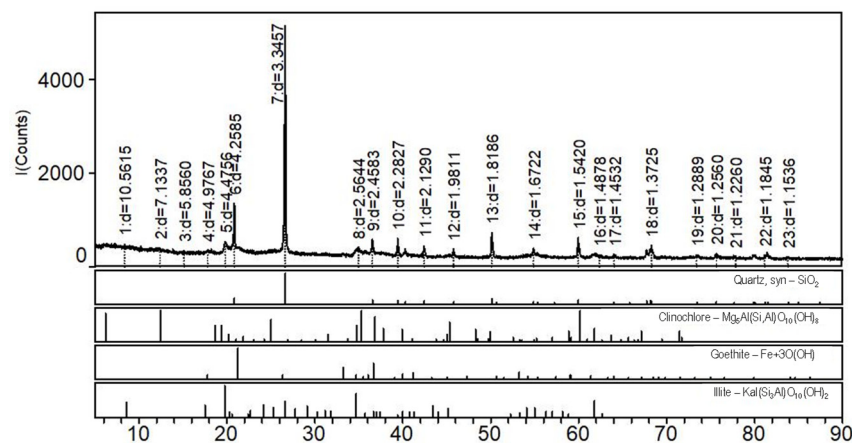| Specific Gravity	Maximum Dry Density/g·cm³	Optimum Moisture Content/%	Liquid Limit/%	Plastic Limit/%	Plasticity Index	Proportion/%		
						Particulate 0.075~2 mm	Powder Particle 0.075~0.005 mm	Clay Particle <0.005 mm
2.68	1.54	27.5	53.4	32.7	20.7	7.53	50.10	42.37

Figure 1. X-ray diffraction pattern of red clay.

2.2. Experimental Method

In this experiment, clay, lignin fiber, and lime were used as modifiers to research the disintegration characteristics and microstructure of red clay. According to the disintegration device in Reference [18], the test device is improved. To count accurately and conveniently, the intelligent dynamometer is used to replace the traditional cylinder. The new device is shown in Figure 2. The disintegration soil sample is prepared by the pressure sample method, and the sample is a cube with a side length of 5 cm. Each layer of soil is compacted and shaved, and compacted by hoisting jack. The chemical element composition and content of clay, lignin fiber and lime were determined by XRF analysis. The measurement time was 200 s. Each standard sample was measured three times. The high voltage and current of the X-ray tube were 20 kV and 0.45 mA, respectively. The number of energy spectrum channels was 2048. The analysis results are as follows: lignin fiber (particle size < 0.5 mm, white, thin strip, humidity < 3%), clay (particle size < 0.005 mm, with the clay mineral content as high as 64.7%) and lime (CaO: 92.49%, MgO: 5.22%, SiO_2: 0.65%, others: 1.15%); these are selected as modifier materials. This paper analyzes the effects of three modifiers on the disintegration of red clay from the aspects of physical and chemical modification. Three experimental groups, single clay, single lignin fiber and single lime are set up, as well as the raw soil, without adding modifiers, as the control group. In each group, four different incorporation ratios (percentage of dry soil quality) are set up, which are 2%, 4%, 6% and 8%, respectively. In order to reduce the influence of other factors and ensure the accuracy of the analysis data, three parallel samples are made for each group of

tests, a total of 39 samples. The method of configuring the test soil is as follows: a certain mass of dry soil is taken out and sieved for later use. According to the experimental plan, a certain amount of clay, lignin fiber and lime is weighed. Then the modifier and soil are mixed and stirred evenly, and water is added and stirred until the optimal moisture content is reached. The optimal moisture content refers to the moisture content at the maximum dry density that can be achieved under standard compaction conditions for the same kind of soil. The dry density of the sample is 1.39 g/cm^3. The water used in the experiment was Guilin rainwater, and the pH value of Guilin precipitation ranged from 3.72 to 7.66, with an average of 4.80, which was acidic.
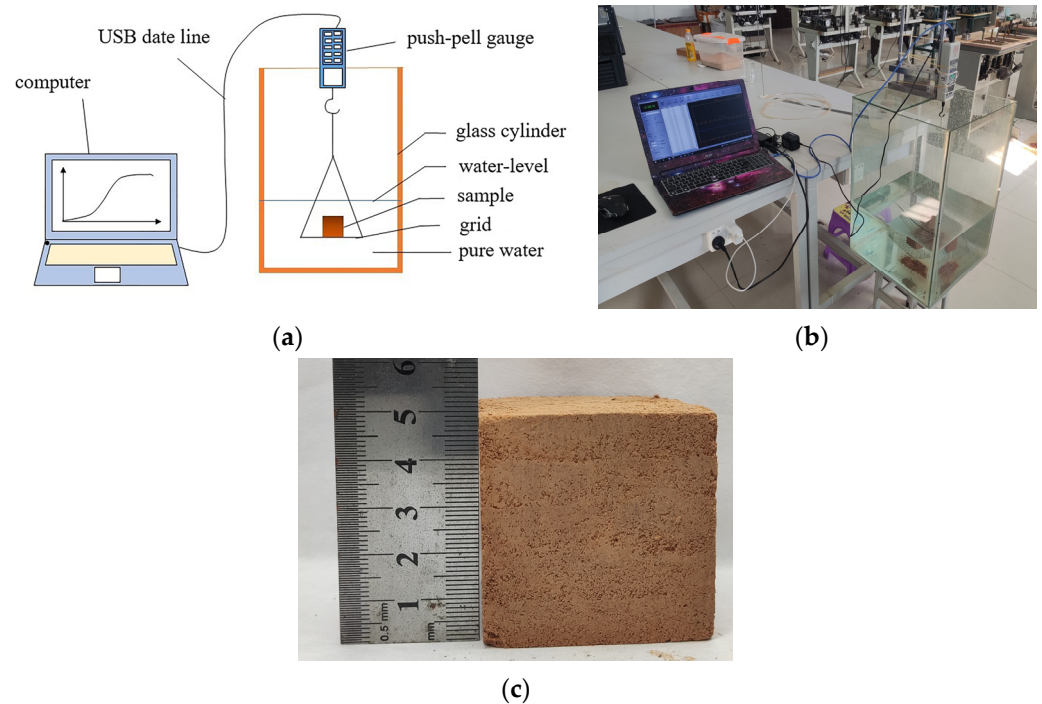

Figure 2. Test equipment and samples. (**a**) Equipment sketch, (**b**) equipment sketch, (**c**) disintegrating sample.

3. Experiment Results and Analysis

3.1. Test Disintegration Phenomenon

By all accounts, many small bubbles will escape from the surface pores when the reshaped specimen is immersed in water. Cracks appear on the soil surface, and the width of the cracks gradually increases. With the soil sample producing granular and flaky droplets, the water gradually becomes turbid. The edges of the crack then collapse into lumps. The soil sample gradually flakes off in the form of small particles, fragments, and clumps until it completely disintegrates. The soil disintegration phenomenon is shown in Table 2.

The samples with lignin fiber content of 0% and 2% are taken as an example, as shown in Figure 3. The disintegration phenomenon of reshaped red clay before and after adding lignin fiber is shown: the disintegration time of lignin fiber-doped soil was short and the disintegration was rapid. The soil block was broken down into finer particles and the sample gradually disintegrated from the surface to the interior. During the disintegration process, bubbles were continuously generated and the water quality was turbid. The soil without lignin fibers disintegrated relatively slowly. The water was clearer and there were fewer bubbles escaping from the pores. The disintegration block was large and the disintegration time was long.

Table 2. Soil disintegration phenomenon.

| Modifier	Disintegration Characteristic	Initial Demise	Soaking Time
Control group	After soaking in water, a large number of bubbles escaped; the early disintegration was slow, the soil fell off in a block form, and the soil collapsed to the later stage. The soil accumulated on the grid, slowly disintegrated, and the water quality was clear.	Rapidly	Less than 20 min
Lignin fiber	After soaking, it immediately disintegrated, and the soil properties were loose. There was no obvious crack, and the soil fell in the form of debris. The continuous small-diameter bubbles escaped at a constant speed, the disintegration was complete, and the water quality was turbid.	Rapidly	Less than 13 min
Clay	After soaking, large-diameter bubbles escaped. There were obvious cracks and soil blocks scattered. When the disintegration was complete, the water quality was cloudy.	Faster	Less than 25 min
Lime	After soaking, a small number of large-diameter bubbles escaped. The cracks were obvious and continued to develop, and the surface collapsed into small-granular soil. Disintegration was slower, and the water quality was clear.	Slower	Less than 60 min

0 min   4 min   7 min   9 min

(**a**)

0 min   4 min   7 min   9 min

(**b**)
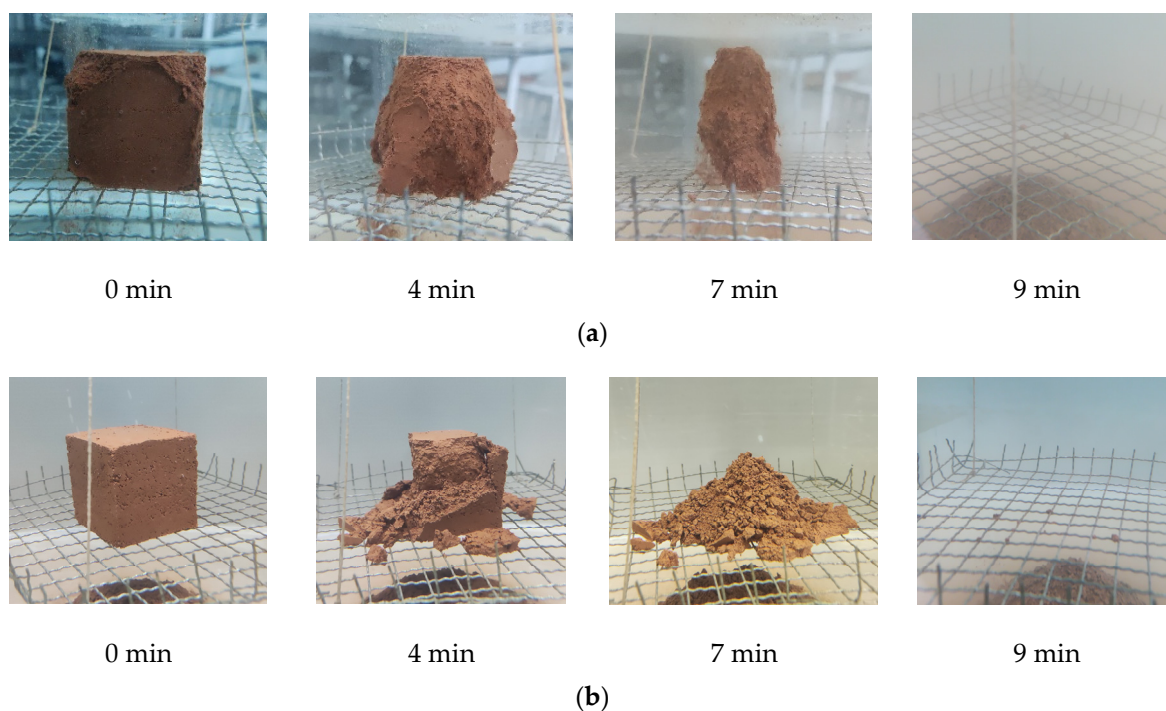
Figure 3. Disintegration process of reshaped red clay samples. (**a**) The disintegration process of reshaped red clay mixed with 2% lignin fiber. (**b**) The disintegration process of remolded red clay without lignin fiber.

3.2. Effect of Modifier on Disintegration Curve of Red Clay

The average disintegration rate refers to the ratio of the total amount of disintegration to the time of the whole disintegration process in the process of soil disintegration, which reveals the average rate characteristics of soil disintegration. The disintegration curve of reshaped red clay by lignin fiber is shown in Figure 4. It can be seen from Figure 4 that the initial disintegration rate of the modified soil with lignin fiber is small, and the

disintegration rate in the middle and late stages is large. The content of lignin fiber decreases from 2% to 0%, and the disintegration time decreases from 17 min to 8 min. With the average disintegration rate increasing, the anti-disintegration of the soil decreases. When the disintegration rate reaches more than 60%, the disintegration time of soil without a modifier is the longest. This is because when not cured, the incorporation of lignin fibers results in changes in the internal pores of the sample. And in the short term, there is no good cross-stacking effect between the soil particles and the fibers inside the sample. With the lignin content increasing, the cementing material continues to wrap the silt particles, gradually forming larger particles, resulting in larger pores between the particles; some excess lignin cannot be mixed with silt to form cementing material, so it cannot play the role of wrapping, covering and pore filling [20]. The pores generated by the fiber penetrate from the surface of the sample to the inside of the sample. Water easily immerses the soil, resulting in an increase in soil disintegration. The soil collapses rapidly after immersion and the water stability is reduced. While the lignin fiber content increases from 2% to 8%, the disintegration time of the soil increases and the average disintegration rate decreases gradually. This is because the lignin fiber is a filamentous fiber material and it has a certain hydrophilicity [21]. When the amount of fiber is low, the distribution in the soil is not uniform, resulting in the development of soil cracks and the decrease in cohesion. With the increase in lignin fiber content, the soil is subjected to fiber cross-binding, and the structure is relatively stable [22]. In addition, lignin fiber also has certain hydrophilicity, which improves the disintegration resistance of soil, to a certain extent [23].
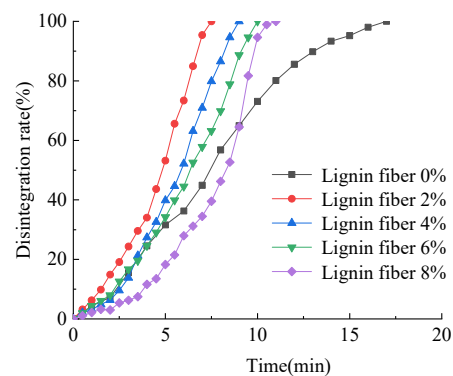
(a)
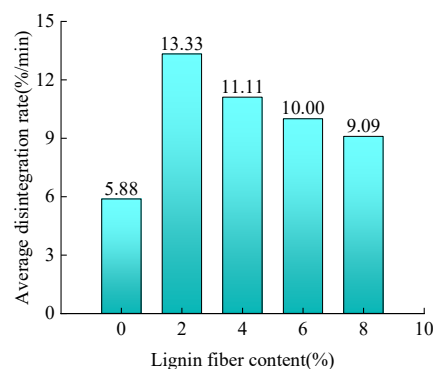
(b)

Figure 4. The disintegration curve of lignin fiber-modified red clay. (**a**) Relationship between disintegration time and disintegration rate. (**b**) Relationship between lignin fiber content and average disintegration rate.

In summary, we can see that the increase in lignin fiber content can slow down the disintegration rate of the soil, and the water sensitivity has been reduced, to a certain extent. However, compared with the undoped lignin fiber, the anti-disintegration resistance is

reduced. It shows that the addition of lignin fiber alone will reduce the water stability of the soil.

Clay is composed of fine soil particles, with a particle size of less than 0.005 mm [18]. The smaller the particle size, the larger the specific surface area, and the more easily the agglomeration. It can be seen from Figure 5a that when the clay content increases, the disintegration time of the reshaped red clay increases, and the water stability of the soil increases. In the whole process of disintegration, the soil disintegration rate is smoothed out, and there is no obvious mutation point in the disintegration process. The average disintegration rate of reshaped red clay is reduced from 5.88%/min to 5.56%/min by adding 2% clay. It shows that the average disintegration rate of soil decreases with the increase in clay content, as shown in Figure 5b. The existence of contact force between particles plays a vital role in the overall stability of the structure. This contact force forms an interconnected bond between particles, thereby constructing a stable structural system. This phenomenon is academically called 'force chain'. However, when the soil sample is immersed in water, the continuous movement of water molecules will destroy the formed force-chain structure in the soil, resulting in damage to the stability of the soil, which in turn leads to the wetting and disintegration of the soil [24]. In addition, salinity in soil is also one of the important factors affecting soil disintegration [25]. When the clay content is high, the number of fine particles in the disintegrated soil is greater. The closer the particles are arranged between each other, the greater the interaction between the particle molecules [26]. The stronger the cementation action between particles, the stronger the disintegration resistance of the soil [27]. In acidic aqueous solution, free iron, aluminum and silica gel will be adsorbed together to form an electric double layer. By binding water to form a micelle, the micelle cements the structural unit into a larger aggregate [28]. In addition, the crystallization of some crystalline minerals also leads to the crystallization connection between the structural units. Thus, a larger aggregate can be formed step by step, thus forming a blocky red clay with high dispersion and overall cementation. For reshaped red clay, there are many cracks of different sizes in the soil. After adding clay particles, cracks can be filled and the density of the soil can be increased. By reducing the number of cracks and slowing down the soaking of the water, it can appropriately increase the water stability of the soil.
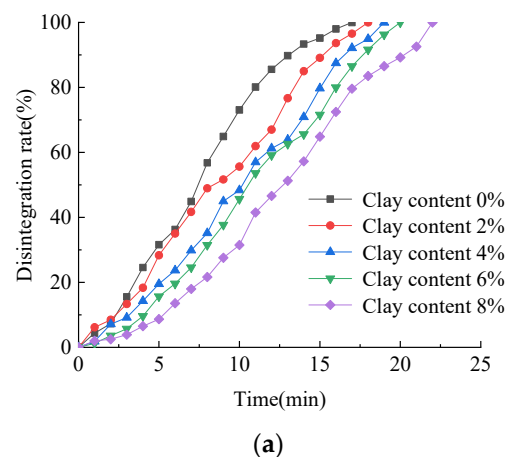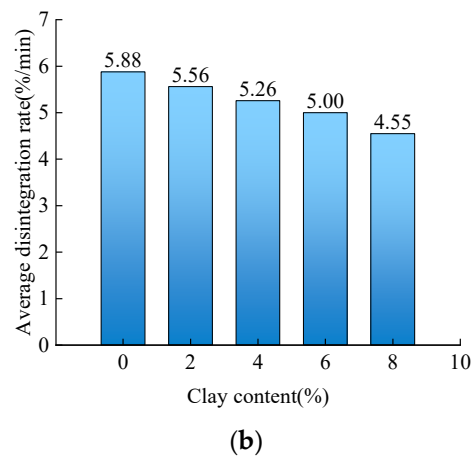

(**a**)

Figure 5. *Cont*.

(b)

Figure 5. Disintegration curve of clay-modified red clay. (**a**) Relationship between disintegration time and disintegration rate. (**b**) Relationship between clay content and average disintegration rate.

The disintegration time of soil modified by lime increases with the increase in lime content. The amount of disintegration is 100%, and the disintegration is complete. The disintegration time of lime content from 0% to 8% is 17 min, 41 min, 44 min, 47 min and 54 min, respectively. The disintegration time increases with the increase in lime content, which is 1.41 times, 1.59 times, 1.76 times and 2.18 times higher than that of the sample without lime. It shows that the incorporation of lime can improve the disintegration resistance of soil. The reason may be that the hydration products of lime agglomerate at the pores of soil particles due to the addition of lime. Only part of the hydrated lime $Ca(OH)_2$ in the lime-stabilized soil is ion-exchanged, and most of the saturated $Ca(OH)_2$ can crystallize by itself and cement the soil particles into a whole. This increases the bonding effect between soil particles and enhances the integrity of soil [29]. Lime effectively improves the water stability of the soil. Lime reacts with active silicon oxide and alumina in soil to form water-bearing calcium silicate and calcium aluminate, which gradually harden under the action of water [30,31]. Therefore, it can be concluded that lime can slow down the immersions of soil into water and improve the anti-disintegration of the soil. In addition, lime can change the microstructure of clay minerals, causing changes in the engineering properties of the soil. In summary, the disintegration of red clay modified by lime has been greatly improved, and the cementation and water stability have also been greatly improved [32,33] (Figure 6).
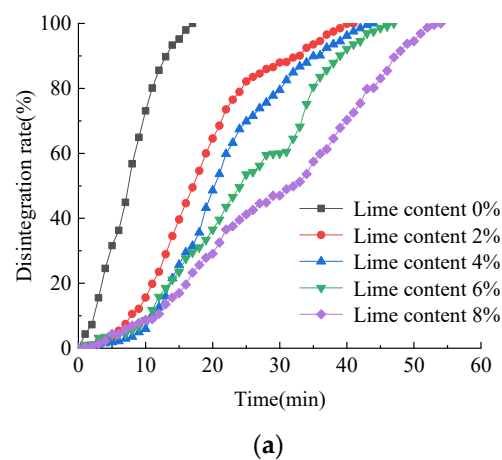

(a)

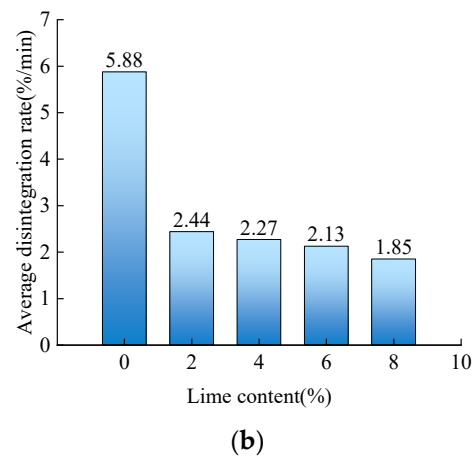**Figure 6.** *Cont.*

(b)

Figure 6. Disintegration curve of lime-modified red clay. (**a**) Relationship between disintegration time and disintegration rate, (**b**) relationship between lime content and average disintegration rate.

3.3. Effect of Modifier on Microstructure of Red Clay

From the electron microscope scanning of red clay in Figure 7, the internal structure particles of raw soil are arranged uniformly, and the number of cracks and micropores small and fewer. The particles mostly contact in the form of point–point, and the pore morphology is diverse. Figure 8 shows the micro-bond contact model and scanning electron microscope of the soil with 2% lignin fiber. In the micro-bond contact model, black lines and brownish yellow blocks represent lignin fibers and soil particles, respectively. After doping with lignin fiber, the reshaped soil is a porous structure, and the large-particle skeleton structure is more obvious. There are few mineral cements between particles, and the particles are dispersed. It shows that the existence of lignin fiber accelerates the development of cracks, and a crack provides a smooth channel for water flow. Lignin fiber acts as a 'bridge' between pores, and thus the anti-disintegration of modified soil shows greater tensile strength [34]. After the incorporation of lignin fiber, the soil particles become coarse, and the fine particles are distributed around the large particles. The proportion of pores increases significantly, which reduces the cohesion, although with the increase in lignin fiber content, the reinforcement effect is enhanced, and the anti-disintegration ability of the soil is improved. However, compared with raw soil, the anti-disintegration ability of soil through modified lignin fiber decreased.
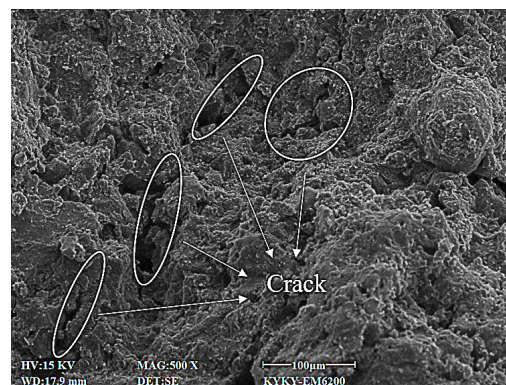

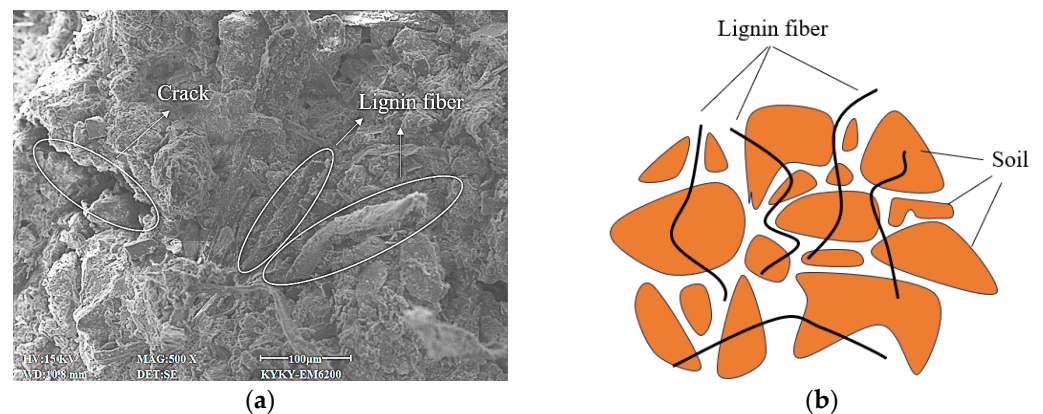**Figure 7.** Raw-soil scanning with electron microscope by 500 times.

Figure 8. Micro-bond contact model and SEM of 2% lignin-fiber red clay. (**a**) 500 times, (**b**) micro-bond model.

The microstructure diagram of reshaped soil mixed with clay is shown in Figure 9. Granular or flaky clay minerals can be seen through the crack grooves. The clay is randomly arranged and distributed among the soil; some is attached to the surface of the soil particles, and some is filled with particle gaps. The soil gap becomes smaller, and there is no through-gap between the soil [35]. The local amplification of Figure 9a is shown in Figure 9b. Under the high-magnification microscope, the clay covers the surface of the soil and fills in the pores. Most of its shape is scaly or granular. Hydrogen bonds are formed between the clay molecules and water molecules in the soil [36]. This hydrogen bond can strengthen the interaction between the soil and the water molecule. It makes the clay particles have strong hydrophilicity and effectively improves the integrity of the soil. Figure 9c shows a microscopic bonding model, which intuitively shows that the clay changes the pore width and enhances the interaction forces within the soil. Natural soil has many cracks, a loose structure, and small cohesion between particles. The addition of clay not only changes the size of the gap between the red clay, but also enhances the cementation and anti-disintegration ability of the soil [37]. It shows that the essence of incorporating clay is in recombining the microstructure of red clay. The cementation formed by the combination of clay and soil enhances the cementation effect. The interaction force between particles increases, which can effectively resist water soaking and enhance the anti-disintegration ability of the soil.
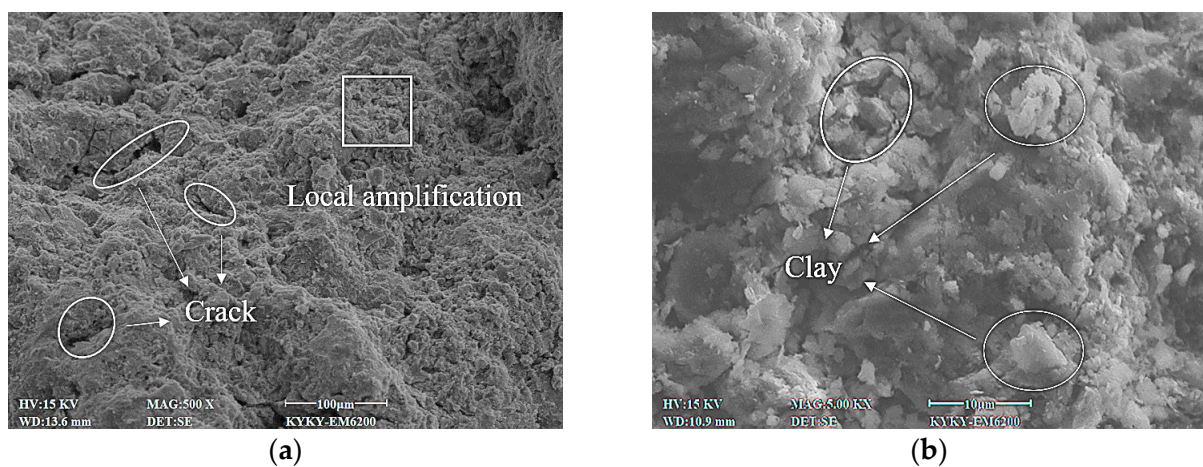

Figure 9. *Cont.*
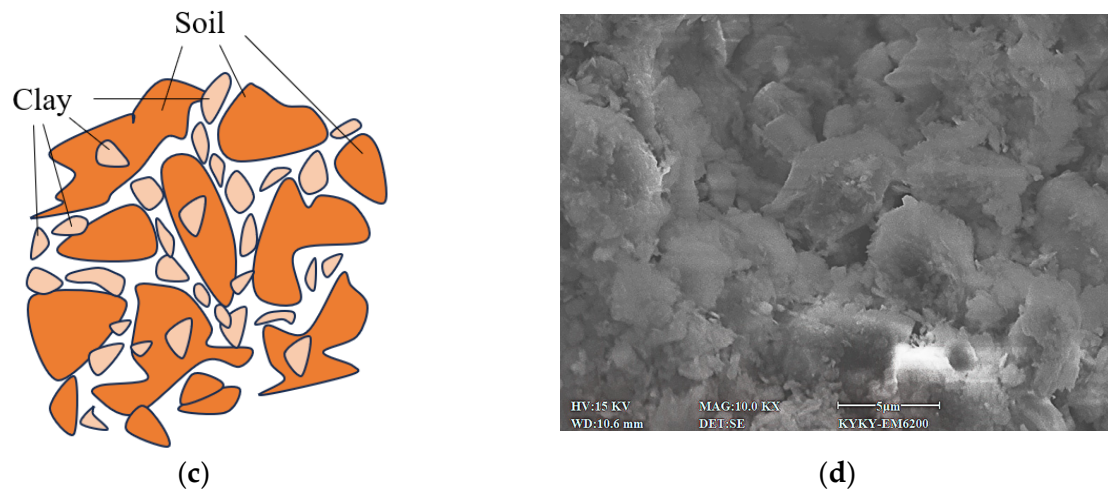
(**c**)

(**d**)

Figure 9. Micro-bond contact model and SEM of 2%-clay red clay. (**a**) 500 times, (**b**) 5000 times, (**c**) micro-bond model, (**d**) clay particles magnified 10,000 times.

Lime reacts with water to form hydration products. The main hydration products of materials are hydrated calcium silicate (C-S-H) and hydrated calcium aluminosilicate silicate (C-A-S-H), which are cementitious. They can fill the soil gap and enhance the bonding force between soil particles [31]. The local amplification of Figure 10a is shown in Figure 10b. Figure 9d is the microstructure of clay after 10,000 times magnification. By scanning electron microscopy magnifying the clay 10,000 times, it can be observed that the hydration products present a gray–white sheet structure in the soil and attach to the surface of the soil, as shown in Figure 10. Lime has excellent water stability and caking ability [30]. With the increase in lime content, the hydration products increase, which can effectively reduce the pore size and quantity. As shown in Figure 10, the surface of the soil sample is smooth and the soil particles have no penetrating cracks. The mineral particles are randomly arranged. A plate-like aggregate is formed by the overlapping of the layered clay mineral wafers with large crystals in the form of surface contact, with a clear boundary. The hydration products are randomly distributed in the soil and remain in the soil in the form of bonding or coating soil particles, and filling gaps. Lime enhances the interaction between soil particles, and the soil particles are arranged more closely [38,39]. Therefore, the soil structure is more stable and more resistant to disintegration.
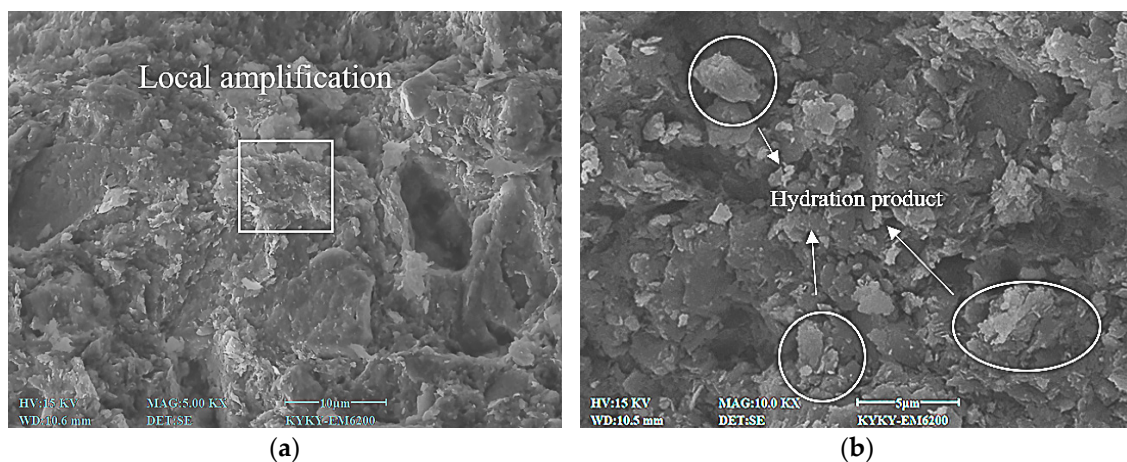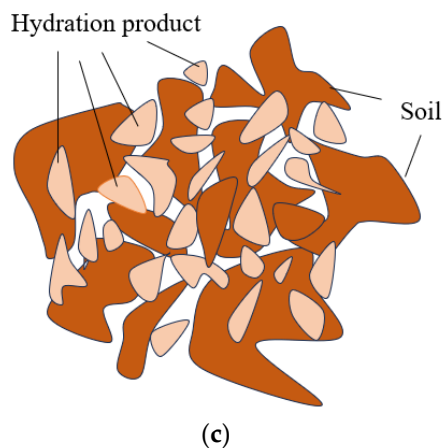

(**a**)

(**b**)

Figure 10. *Cont.*

(**c**)

Figure 10. Micro-bond contact model and SEM of 2%-lime red clay. (**a**) 5000 times, (**b**) 10,000 times, (**c**) micro-bond model.

3.4. Effect of Modifier Types on Saturated Moisture Content of Red Clay

Saturated moisture content θ_s means that when the soil reaches saturation, the pores in the soil are all filled with water. The pore water is continuous and uniformly distributed, and the substrate suction in the soil is zero. The content of the hydrophilic minerals and the pore structure in the soil have a significant effect on the soil–water characteristic curve [40]. The saturated moisture content of different modifier soils is shown in Figure 11. When the lignin fiber content is 2%, its θ_s is 43.68%. And its saturated moisture content is higher than that of raw soil. When the lignin fiber content increased from 2% to 8%, the saturated moisture content increased from 43.68% to 48.91%. The saturated moisture content depends on the pore structure of the soil, and the smaller the pore size, the lower it is. The saturated moisture content of reshaped soil increases with the increase in lignin fiber content. This shows that the porosity of the soil is increased by the lignin fiber.

When the clay content is 2~8%, the θ_s increases from 42.05% to 43.91%. The saturated moisture content gradually increases with the increase in its content. But the rate of increase has been slow. When the content of hydrophilic minerals is high, the soil shows greater suction and higher saturated-moisture content [41]. It reflects the higher hydrophilic-mineral content and the smaller pore size. The pore structure tends to be compact and the compactness is promoted. With the increase in clay content, the clay particles are uniformly distributed in the soil, and the contact area between clay minerals and soil particles is increased. In addition, the clay has a certain hydrophilicity [42], so the saturated moisture content is increased.
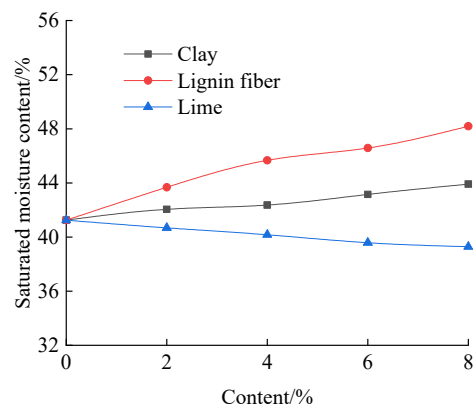

Figure 11. Saturated water content of red clay.

Compared with lignin fiber and clay, the saturated moisture content of the lime content decreased gradually. The reason for this phenomenon is that lime reacts with

water and carbon dioxide to form hydrated calcium silicate (C-S-H) and hydrated calcium aluminosilicate silicate (C-A-S-H) [31]. These hydrated substances coat soil particles and fill pores. As a result, the pores in the soil are reduced or filled, and the saturated water content is reduced. Therefore, the relationship between the porosity of the three modifiers can be obtained: the porosity of lime soil is small, the porosity of lignin fiber is the largest, and the porosity of clay is in the middle.

3.5. Microscopic Porosity Analysis

In addition to external factors, the occurrence of rock disintegration is more important for the influence of its internal pore structure [43,44]. Based on the damage theory of pores, this paper analyzes the difference in disintegration of reshaped red clay mixed with three modifiers from the microscopic viewpoint. The scanning electronic microscope and the disintegration time of the three modifier-reshaped soils are shown in Figures 12 and 13, respectively. Under the same magnification of 2000 times, there are obvious gaps in the microstructure of the lignin fiber soil. The particles are obvious and the angularities are clear. Compared with lignin fiber, the number of pores in the clay soil decreases. this shows that the addition of clay can effectively reduce the number of micropores, and can effectively reduce the pore area. Compared with the previous modifier, the number of pores in the lime soil is the least. The particles are in close contact with each other, and the skeleton has no penetrating cracks.
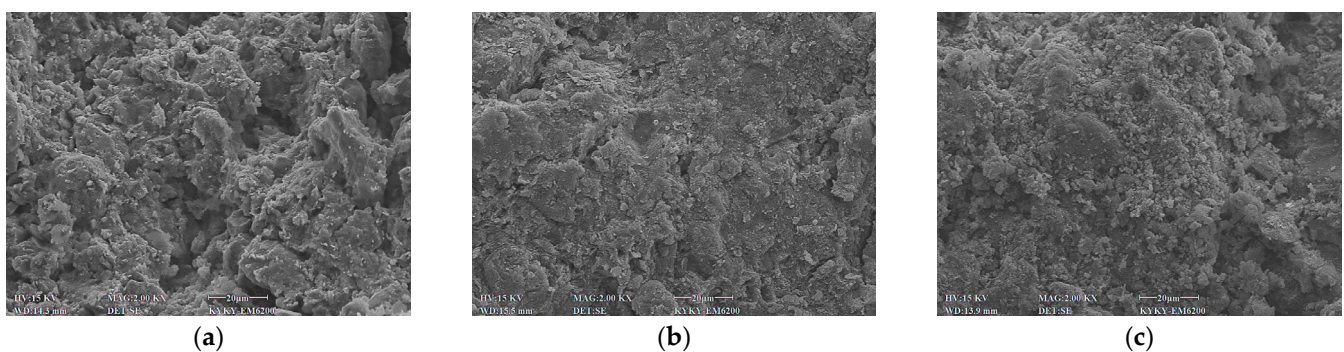
(**a**)   (**b**)   (**c**)

Figure 12. Microstructure of three modifiers with 4% content. (**a**) Lignin fiber, (**b**) clay, (**c**) lime.
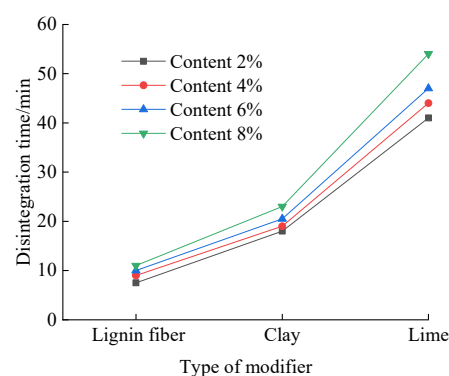
Figure 13. The disintegration-time curves of different admixtures with 4% content.

In addition, this paper also uses X-ray to scan the fault surface of the sample to analyze the pore size inside the sample. The processed image is binarized, and the processed image is divided into black and white parts, and the black part is the pore. It can be seen from Figure 14 that the black part of the lignin-doped fiber sample is the greatest and the pores are the largest. There are only some cracks in the clay-doped sample, and the number of pores is reduced. The binary image of the lime-doped sample has no penetrating cracks, and there are only tiny pores between the soil particles. It can be seen from this that the number

of pores of the lime-doped sample are the least, followed by the clay-doped sample, and the number of pores in the lime-doped sample is more than that of the lignin-doped fiber.
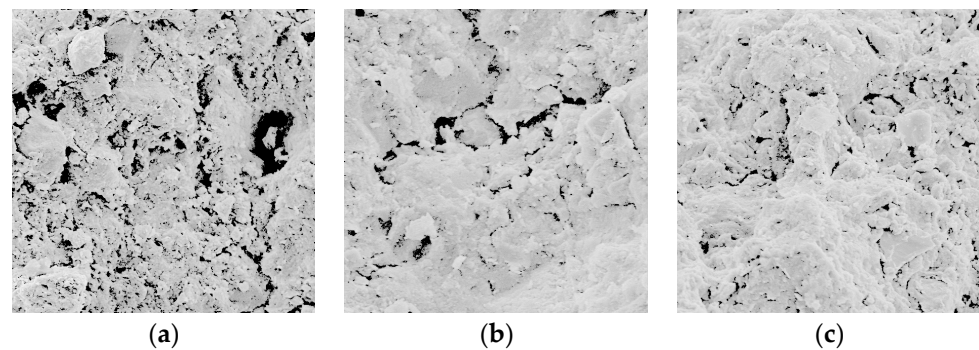

| (a) | (b) | (c) |

Figure 14. Section image after binarization. (**a**) Lignin fiber, (**b**) clay, (**c**) lime.

The destruction process of rocky soil is essentially the expansion process of micro-cracks. According to the principle of fracture energy consumption, the propagation path of the fracture always follows the weak-strength surface [45]. That disintegration is the immersion in water, resulting in fracture development. Under the action of water stress, the internal stress of the soil dissipates, and the soil collapses. The contact interface between the particles inside the soil, that is, the pore size, provides a channel for the disintegration of the rocky soil [46]. At the same time, the pore size determines the disintegration ability of the three admixtures to the reshaped soil. The relationship between the pore volume of the three reshaped soils is as shown in Equation (1):

$$V_1 > V_2 > V_3 \tag{1}$$

where V_1 is the pore volume of lignin fiber-reshaped soil;

V_2 is the pore volume of clay-reshaped soil;

V_3 is the pore volume of lime-reshaped soil.

The porosity n in the soil is as shown in Equation (2):

$$n = \frac{V_{pore}}{V_{soil}} \tag{2}$$

where V_{pore} is the volume of pore;

V_{soil} is the volume of soil sample.

Therefore, when the volume of the sample is the same, the porosity of the reshaped soil of the three admixtures is as shown in Equation (3):

$$n_1 > n_2 > n_3 \tag{3}$$

where n_1 is the porosity of lignin fiber-reshaped soil;

n_2 is the porosity of clay-reshaped soil;

n_3 is the porosity of lime-reshaped soil.

Combined with the previous analysis, the disintegration time of lignin fiber is the shortest and the average disintegration rate is the largest. Therefore, the larger the porosity, the lower the anti-disintegration ability. Meng Xiangxi [47] obtained the damage constitutive model relationship constructed by porosity.

$$D_n = \frac{n - 0.01}{0.99} \tag{4}$$

where n is the porosity of soil at different times;

D_n is the damage factor, with porosity as the damage variable.

The relationship between porosity and damage factor of three different modifiers is obtained by combining Equations (3) and (4), as follows:

$$D_1 > D_2 > D_3 \tag{5}$$

where D_1 is the damage factor of lignin fiber soil;

D_2 is the damage factor of lignin fiber soil;

D_3 is the damage factor of lignin fiber soil.

According to the information revealed by Formula (5), we can clearly see that the wood fiber-remolded soil shows the largest damage factor, followed by the clay-remolded soil, while the lime-remolded soil shows the smallest damage factor. Combined with the above pore damage analysis, we can draw a clear conclusion: there is a positive correlation between the porosity of the soil and its damage factor; that is, the higher the porosity, the greater the damage factor, which further leads to a significant decrease in the mechanical properties of the soil [48,49], and the ability to resist disintegration is also weakened. Therefore, under the same conditions, the lignin fiber-remolded soil exhibits the lowest anti-disintegration ability. Considering the influence of the binding correlation between the admixture and the red clay on the initial porosity of the sample, we can further infer that this effect can determine the size of the damage factor. In summary, the microscopic damage of pores is one of the key factors that determine the disintegration ability of soil. It can be seen from the above research that the addition of lime significantly improves the anti-disintegration ability of the soil, which in turn strengthens the resistance of the soil to softening and disintegration. At the same time, the improvement from the lime also significantly enhances the water sensitivity of the soil, so that it can maintain more stable physical and mechanical properties in the face of water changes. Therefore, the use of lime to improve the soil can not only effectively improve the utilization rate of the slope and foundation soil, and optimize the allocation of land resources, but also significantly reduce the economic cost of maintenance projects and achieve a win–win situation of economic and ecological benefits. The research results have important academic value and practical significance for deepening the understanding of soil improvement technology, promoting the sustainable utilization of land resources and the protection of the ecological environment.

4. Conclusions

The wetting disintegration test of red clay in the Guilin area was carried out. The disintegration characteristics of red clay with lime, lignin fiber, and clay at the same content of 0%, 2%, 4%, 6% and 8% were studied. The soil–water characteristic curves of red clay reshaped by different modifiers are obtained. By analyzing the test results, the main conclusions are as follows:

1. After adding lignin, the water-holding capacity of red clay decreases, the anti-disintegration ability of soil decreases, and the water stability decreases. The water sensitivity of red clay is improved after adding clay, and the disintegration time increases with the increase of clay content. The water-holding capacity of red clay increases after structural lime treatment, and this water-holding capacity increases with the increase in its content. Comparing and analyzing the anti-disintegration ability of the three modifiers, lime can effectively improve the immersion of red clay in water, and the water stability is improved.

2. The incorporation of lignin fiber leads to the change in the internal pores of the sample; in the short term, there is no good cross-accumulation effect between the soil particles and the fiber in the sample, and the water easily immerses the soil, which leads to the decrease in the anti-disintegration ability of the soil. The clay particle size is small, and it is incorporated into the soil to fill the pores of the soil. The cementation of clay minerals in the clay particles enhances the disintegration resistance of the soil, and the disintegration time increases with the increase in clay content. The hydration of lime

changes the original pore structure and material composition of red clay and improves the disintegration of the red clay.

3. The content of water-soluble minerals and the pore structure of the soil have a significant effect on the soil–water characteristic curve. In red clay, with the increase in wood fiber content, the saturated water content gradually increased from 43.68% to 48.91%, showing a significant upward trend. This change reflects the effect of wood fiber incorporation on the water-holding capacity of red clay. In contrast, the saturated water content of red clay increases slightly with the increase in clay content, which may be related to the specific properties of clay adsorption in water. On the other hand, the incorporation of lime will lead to a decrease in the number of pores in the internal structure of red clay, thus reducing its saturated water content. This finding reveals the modification effect of lime on the pore structure of red clay and its effect on water retention capacity.

4. After comparing the saturated water content of the three additives, it was found that the porosity of lignin-remolded soil was the highest, followed by clay-remolded soil, and lime-remolded soil was the lowest. The damage analysis showed that the damage factor was negatively correlated with the disintegration resistance. The damage factor of lignin-remolded soil was the largest and the disintegration resistance was the worst. Clay-remolded soil was second; the lime-remolded soil had the smallest damage factor and the best disintegration resistance.

References

1. Zhang, Y.H.; Gao, Q.F.; Yu, G.T.; Zhou, Q.S.; Cao, S.P. Water Retention and Strength Properties of Red Clay Containing Cracks. *Sci. Technol. Eng.* **2023**, *23*, 5278–5284.

2. Yang, E.J.; Zeng, S.S.; Mo, H.Y.; Yang, C.L.; Chen, C.; Wang, Y.F. Analysis of the Mineral Compositions of Lateritic Clay in Guangxi and their Influence. *Adv. Mater. Sci. Eng.* **2022**, *2022*, 4068773. [CrossRef]

3. Ilyas, A.; Shahid, A. Determination of collapse and consolidation behavior of cohesionless soils. *Bull. Eng. Geol. Environ.* **2022**, *81*, 458–475.

4. Zhang, S.; Xu, Q.; Hu, Z. Effects of rainwater softening on red mudstone of deep-seated landslide, Southwest China. *Eng. Geol.* **2016**, *204*, 1–13. [CrossRef]

5. Fu, J.W.; Yang, J.M.; Guo, H.C.; Zhang, F. Study on rock mechanics response and permeability characteristics of crack grouting under hydraulic-mechanics coupling. *GOLD* **2023**, *44*, 12–17.

6. Jia, D.Q.; Pei, X.J.; Zhang, X.C.; Zhou, L.H. A test study of the microscopic mechanism of modified glutinous rice mortar solidified loess. *Hydrogeol. Eng. Geol.* **2019**, *46*, 90–96.

7. Wu, J.H.; Ren, M. Effect of hydroxypropyl methyl cellulose as soil modifier on solute migration in soil. *Trans. Chin. Soc. Agric. Eng.* **2019**, *35*, 141–147.

8. Wu, J.H.; Tao, W.H.; Wang, H.Y.; Wang, Q.J. Influence of sodium carboxyl methyl cellulose on soil aggregate structure and soil water movement. *Trans. Chin. Soc. Agric. Eng.* **2015**, *31*, 117–123.

9. Feng, R.Y.; Wang, H.J.; Guo, F.; Yang, Y.; Che, L.; Gu, X.H.; Chen, W.L. Effects of Modified Straw Soil Amendment on Soil Structure and Water Characteristics. *J. Irrig. Drain.* **2015**, *34*, 44–48+65.

10. Shang, Y.N.; Hu, F.N.; Zhao, S.W.; Huo, N.; Chang, W.Q. Effects of Cementing Materials on the Formation of Loessial Soil Aggregates. *J. Soil Water Conserv.* **2017**, *31*, 204–208+239.

11. Zhang, Y.; Feng, H.; Wang, Y.K.; Du, J.; Zhao, X.N.; Xu, X.P.; Wang, Y. Preliminary Research on Moisture Characteristic of New Soil Conditioner and its Influences on Seeding Stage of Corn. *Water Sav. Irrig.* **2008**, *5*, 6–9.

12. Zhang, S.; Tang, H.M. Experimental study of disintegration mechanism for unsaturated granite residual soil. *Rock Soil Mech.* **2013**, *34*, 1668–1674.

13. Chen, S.-M.; Yilmaz, E.; Wang, W.; Wang, Y.-M. Curing stress effect on stability, microstructure, matric suction and electrical conductivity of cementitious tailings backfills. *Constr. Build. Mater.* **2022**, *360*, 1–10. [CrossRef]

14. Wang, T.; Hu, B.; Liu, J.; Chen, P.Z. Experimental Study on Shear Strength of a Root-Soil Composite of a Modified Expansive Soil. *Soil Eng. Found.* **2023**, *37*, 835–840.

15. Chen, W.H.; Qu, S.H.; Lin, L.B.; Luo, Q.; Wang, T.F. Ensemble Learning Methods for Shear Strength Prediction of Fly Ash-Amended Soils with Lignin Reinforcement. *J. Mater. Civ. Eng.* **2023**, *35*, 22–37. [CrossRef]

16. Hu, X.Q.; Hong, L.; Xu, G.L.; Yang, X.; Jiang, G.W. Impacts of Fiber Content and Fiber Length on the Strength and Deformation of Fiber Reinforced Soil. *Saf. Environ. Eng.* **2015**, *22*, 139–143.

17. Liu, J.F.; Su, Y.H. Analyses of the Strength Characteristics of Solidified Desert Aeolian Sandy Soil. *J. Highw. Transp. Res. Dev.* **2017**, *11*, 32–36. [CrossRef]

18. *GB/T 50123-2019*; Standard for Soil Test Method. China Planning Press: Beijing, China, 2019.

19. *SY/T 5163-2018*; Analysis Method for Clay Minerals and Ordinary Non-Clay Minerals in Sedimentary Rocks by X-ray Diffraction. Petroleum Industry Press: Beijing, China, 2018.

20. Zhou, E.Q.; Ju, D.Y.; Cui, L.; Zhang, M.; Zuo, X. Unconfined compressive strength properties of lignin modified silt. *J. Jiangsu Univ. (Nat. Sci. Ed.)* **2023**, *44*, 614–620.

21. Sun, Y.X.; Pang, X.F.; Li, X.Y.; Pang, J.Y.; Su, L. Study on Hydrophilic Modification of Lignin. *China For. Prod. Indusfry* **2020**, *57*, 15–18.

22. Wang, F.C.; Qin, M.Q.; Li, D.; Sun, Q. Experimental Study on Permeability and Disintegration Performance of Carex Root Fiber Soil. *J. Shenyang Jianzhu Univ. (Nat. Sci.)* **2021**, *37*, 287–295.

23. Ye, J.H.; Zhao, Q.L.; Wu, L.; Fu, S.Y.; Ma, K.C.; Xiong, Z.L. Preparation and Hydrophilicity of Lignin/Polyvinyl Chloride (PVC) Membrane. *Chem. Ind. For. Prod.* **2022**, *42*, 95–100.

24. Zhang, X.; Du, D.; Man, T.; Ge, Z.; Huppert, H.E. Particle clogging mechanisms in hyporheic exchange with coupled lattice Boltzmann discrete element simulations. *Phys. Fluids* **2024**, *36*, 013312. [CrossRef]

25. Han, Y.; Wang, Q. Feature and mechanism analysis of dispersive soil disintegration impacted by soil water content, density, and salinity. *Eur. J. Soil Sci.* **2023**, *74*, e13353. [CrossRef]

26. Han, Z.L.; Zhang, L.Q.; Zhou, J.; Wang, S. Effect of clay mineral grain characteristics on mechani-cal behaviours of hydrate-bearing sediments. *J. Eng. Geol.* **2021**, *29*, 1733–1743.

27. Liang, C.Y.; Wu, Y.D.; Liu, J.; Wu, H.J. Influences of arrangement and cementation of soil particles on structure of artificial structural soil. *Chin. J. Geotech. Eng.* **2022**, *44*, 2135–2142.

28. Tang, L.S.; Wang, Y.X.; Sun, Y.L. Test Study on Effect of Free Iron Oxide in Granite Laterite on cementation Characteristics of Laterite. *Ind. Constr.* **2023**, *53*, 137–143.

29. Lu, X.M.; Fen, L.J.; He, N.; Lin, X. Experimental Study on Engineering Characteristics of Cement-Lime-Improving Silt in Eastern Henan Province. *Coatings* **2022**, *12*, 501. [CrossRef]

30. Bian, J.M. Water Stability of Lime-treated Expansive Soil. *J. Yangtze River Sci. Res. Inst.* **2016**, *33*, 77–82.

31. Haas, S.; Ritter, H. Soil improvement with quicklime—Long-time behaviour and carbonation. *Road Mater. Pavement Des.* **2019**, *20*, 1941–1951. [CrossRef]

32. Zhang, X.J.; Liu, P.; Yang, X.Q.; Wang, Y. A Study of the Relationship Between Permeability and Pore Structure of Lime-treated Loess. *J. Guangdong Univ. Technol.* **2021**, *38*, 97–103.

33. Tian, Y.C.; Zhang, H.B.; Wang, Y.L. Study on mechanical properties of carbonation curing fluorogypsum and slaked lime. *J. Funct. Mater.* **2024**, *55*, 2133–2141.

34. Zhao, L.J. Study on Strength and Disintegration Characteristic of Improved Granite Eluvial Soil. Ph.D. Thesis, Hunan University of Science and Technology, Zhuzhou, China, 2015.

35. Li, S.J.; Tao, S.; Wang, Q.F.; Luo, L.F.; Wang, L.Y.; Wan, M.G.; Liu, Q.L. Effect of clay on microstructure and mechanical properties of red clay. *Technol. Innov. Appl.* **2023**, *13*, 45–49+53.

36. Wang, T.L.; Li, Y.L.; Su, L.J. Types and boundaries of bound water on loess particle surface. *Chin. J. Geotech. Eng.* **2014**, *36*, 942–948.

37. Han, Z.F. Molecular Dynamics Study on the Micromechanical Properties of Clay Minerals. Master's Thesis, China University of Mining & Technology-Beijing, Beijing, China, 2020.

38. Wang, L.; Li, X.A.; Zhao, N.; Hong, B. Effect of clay content on physical and mechanical properties of loess soils. *Chin. J. Geol. Hazard Control* **2018**, *29*, 133–143.

39. Wang, Y.J.; Wang, Y.W.; Jin, F.Y.; Ma, T.T. Soil-water Characteristic Curve and Freezing Characteristic Curve of Lime Improved Soil. *J. Disaster Prev. Mitig. Eng.* **2020**, *40*, 967–973.

40. Cheng, Y.L.; Huang, D. Influence of pore structure characteristics on soil-water characteristic curves under different stress states. *Chin. J. Eng.* **2017**, *39*, 147–154.

41. Shao, Y.J.; Shi, B.; Liu, C.; Gu, K.; Tang, C.C. Temperature effect on hydro-physical properties of clayey soils. *Chin. J. Geotech. Eng.* **2011**, *33*, 1576–1582.

42. Wang, C.H.; An, D.; Qu, H.; Han, C.; He, X.H. Influence of the Clay Mineral on Coal Freezing Adhesive Strength of Coal Transportation Equipment. *Non-Met. Mines* **2017**, *40*, 33–36.

43. Li, M.Y. Study of Disintegration and Microstructural Change Patterns under the Action of Water in Soft Rocks of the Xujiahe Formation. Master's Thesis, Southwest Jiaotong University, Chengdu, China, 2022.

44. Zuo, Q.J.; Wu, L.; Luo, T.; Bian, Y.S.; Tan, Y.Z. Macro disintegration characteristics and micro mechanism of slate in the Yaojia tunnel of the Shanghai-Kunming Passenger Dedicated Line. *Hydrogeol. Eng. Geol.* **2015**, *42*, 65–69.

45. Fang, L.; Zhou, H.M.; Zhang, Y.H. Influence of Microcracks on Strength Parameters of Engineering Rock Mass. *Chin. J. Rock Mech. Eng.* **2011**, *30*, 2703–2709.

46. Lu, Y.F.; Hou, K.P.; Sun, H.F.; Sun, W.; Jiang, J. Experimental study on disintegration resistance characteristics of different kinds of schist. *J. Saf. Sci. Technol.* **2022**, *18*, 114–120.

47. Meng, X.X. Basic Experimental Study on the Damage Evolution Rule of Rock Mass under the Action of Water-Rock. Master's Thesis, Shandong University of Science and Technology, Qingdao, China, 2020.

48. Li, W.; Li, S.; Wang, H.Q. Experimental study on internal pore structure and energy dissipation of basalt fiber reinforced concrete under stress damage. *Compos. Sci. Eng.* **2023**, 55–62. [CrossRef]

49. Wu, X.H. Study on Physical and Mechanical Properties and Damage Mechanism of Granite at Different Heating Temperatures after Water-Cooling. Ph.D. Thesis, University of Science and Technology Beijing, Beijing, China, 2022.